The Fine Structural Study of Spermiogenesis in the Freshwater Oligochaete, *Tubifex hattai*, with a Note on the Histone Transition in the Spermatid Nucleus

By

Haruo Jaana

Zoological Institute, Hokkaido University

(With 2 Text-figures, 1 Table and 6 Plates)

The structure and formation of spermatozoa have been studied repeatedly in various species of oligochaetes (Block and Goodnight, 1980; Troyer and Cameron, 1980; Jamieson, 1981; Braidotti and Ferraguti, 1982; etc.). Most of these works have dealt with acrosome morphogenesis (Cameron and Fogal, 1963; Anderson and Ellis, 1968; Shay, 1972; Jamieson et al., 1978) and the shaping of the sperm head (Ferraguti and Lanzavecchia, 1971; Lanzavecchia and Lora Lamia Donin, 1972; Troyer, 1980). In a comparative study of spermatozoa in megascolecid and lumbricid earthworms, Jamieson (1978) have found taxonomic significance in the fine structure of their acrosome and tail flagellum. No similar study, however, has been carried out for a Japanese species of the freshwater oligochaete, *Tubifex hattai*.

According to light microscopic observation of fertilization in *T. hattai* (Hirao, 1968), a conspicuous entrance cone appears at the site of sperm penetration on the egg surface. The fine structural study of fertilization has clarified the formative mechanism of such a cone in the eggs of various marine animals (cf. Epel, 1978). In view of the results of these observations, the acrosome complex of *Tubifex* spermatozoon is expected to play an important role during the sperm entry into the egg. In order to analyze the underlying mechanism of fertilization in *T. hattai*, more knowledge of the fine structure of spermatozoon may be required.

The objective of this study is to provide such detailed information on the fine structure of spermatozoa and to describe the complete process of spermiogenesis in *T. hattai*. In addition, the transition of nuclear proteins during the shaping of the sperm head will be also studied cytochemically. The results are compared to previous observations on other oligochaetes and, where possible, functional interpretations are suggested.

Materials and Methods

The specimens of a freshwater oligochaete, *Tubifex hattai*, were collected in a stream running through the campus of Hokkaido University and cultured in the laboratory with running water for several years. They were fed on a mixture of cornmeal and yeast every week and were propagated all the year round. In worms near oviposition, large oocytes in their ovisac can be observed through the dorsal body wall of the clitellum (Hirao, 1964). The male germ cells are usually found packed in the sperm sacs or suspended in the coelom of Segment X (male segment) of these worms (Jaana, 1982). The worms with large oocytes in their ovisac were collected from the culture and used in this study.

For transmission electron microscopy (TEM), the worms were fixed *in toto* in 5% glutaraldehyde in a 0.1 M cacodylate buffer (pH 7.4) at 0–4°C for 2 hours, at which time each worm was dissected and the clitellar region was removed for analysis. After postfixation in 1% osmium tetroxide in the same buffer for 1 hour at 0–4°C, the specimens were dehydrated in a graded acetone series and embedded in Epon 812. Thin sections were cut on a Porter-Blum MT-1 ultramicrotome and stained successively with uranyl acetate and lead citrate. They were observed in a JEOL JEM-100S electron microscope.

For scanning electron microscopy (SEM), several samples of the clitellar region were removed from the live worms and broken up in a petri dish with the aids of fine needles. The masses of germ cells and the fragments of tissues were rapidly suspended in 5% glutaraldehyde in a 0.1 M cacodylate buffer (pH 7.4) and spread on cover slips previously coated with poly-L-lysine (Mazia et al., 1975). The cover slips bearing the masses of germ cells were gently lowered into a newly prepared glutaraldehyde having the same composition and kept for 2 hours at 0–4°C. The postfixation of samples was carried out by immersing the cover slips in 1% osmium tetroxide in a 0.1 M cacodylate buffer (pH 7.4) for 1 hour at 0–4°C. After dehydration in a graded ethanol series, the samples were critical-point dried in carbon dioxide, sputter-coated with gold and examined in a JEOL JSM-T20 scanning electron microscope.

The basic protein transitions during spermiogenesis were studied cytochemically in light microscopic preparations. For this purpose, the worms were fixed *in toto* in 10% formalin in a 0.2 M phosphate buffer (pH 7.3) at 18–20°C for 6 hours, at which time the clitellar region of each worm was cut away from the body. Paraffin sections 8 μm thick were prepared by the routine method. Cytochemical analyses on spermatids were similar to those used by Bols and Kasinsky (1974), who have characterized the basic nuclear proteins in the mature spermatozoa of cartilaginous fish. Histones were stained by the alkaline fast green (AFG) method (Alfert and Geschwind, 1953). DNA was removed prior to AFG staining with hot (90°C) trichloracetic acid (TCA) or with hot (60°C) picric acid. The deamination or acetylation of lysine residues with nitrous acid (Bloch and Hew, 1960) or with acetic anhydride (Bols and Kasinsky, 1972) were performed to demonstrate the very arginine-rich histones in the nuclei. The specific demonstration of arginine

was carried out by the Sakaguchi reaction modified by Carver et al. (1953).

Results

Spermatozoa singly suspended in the male segment can sometimes be observed by SEM (Fig. 1). Each of them measures about 55 μm long–0.8 μm wide and consists of a head and tail with no clearly differentiated midpiece. About 5 μm of the long head is spearhead-shaped and possesses anteriorly an acrosome whose tip has a swelling (Fig. 1, inset). A remarkable constriction marks the boundary between the head and tail. The tail flagellum is divided into principal and end pieces. Its width is relatively constant throughout the principal piece, measuring about 0.8 μm, but gradually it decreases in the posterior one seventh of the tail length, the end piece. The course of the sperm tail is not straight in fixed specimens but usually shows a characteristic curve immediately behind the head. Furthermore a marked distortion is observed at the position near the posterior end of the principal piece (Fig. 1). Owing to the discrepancy in axes of the head and the tail, each spermatozoon appears as if it possesses a hook in the proximal region of the flagellum.

By TEM, we find that the acrosome existing anteriorly to the nucleus measures about 0.5 μm long and consists of a cap-shaped acrosomal vesicle and an acrosomal tube (Text-fig. 1). The narrow space of the acrosomal vesicle is filled with high electron-dense material. The hollow acrosomal tube is closed anteriorly by the acrosomal veiscle and posteriorly by a deposit of electron-dense material. The elongate nucleus measures about 4 μm in length and contains highly condensed chromatins; there are no apparent fibrous components. Immediately behind the nucleus, there are a pair of mitochondria closely adjoined. This pairing has been often called a nebenkern. Posteriorly to the nebenkern, the spermatozoon possesses a hollow cylindrical centriole from which the tail flagellum extends. The

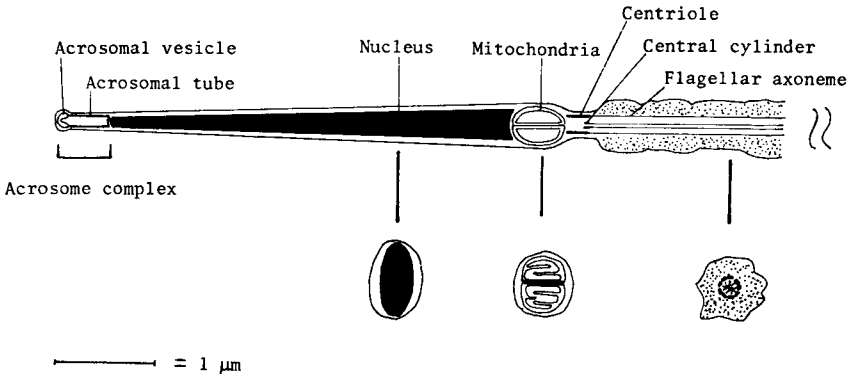

Text-fig. 1. Schematic illustration of the anterior region of *Tubifex* spermatozoon individually suspended in the male segment.

flagellum shows a typical 9+2 arrangement of microtubules. At the anterior terminal of the 2 central singlets, there is a small "central cylinder" which exists in the lumen of the cylindrical centriole. The cytoplasm located in the tail of spermatozoa is relatively large in amount in this species and contains a number of glycogen granules. In the head region, however, the cytoplasm is hardly visible in these spermatozoa; the surface of the elongate nucleus is closely apposed to the sperm plasma membrane.

Mass of spermatids observed by SEM

Like other oligochaetes, the developing spermatozoa of *Tubifex* are connected to a common anucleate mass of cytoplasm or a cytophore. Since a number of spermatids are combined in this manner, the external feature of the cellular mass resembles that of the morula stage embryo. Since the number of spermatids in the mass is hard to determine at the final stages of spermatogenesis, the exact discrimination of early spermatids from spermatocytes is not possible unless the second meiotic division is actually observed in the cellular mass. For this reason the formation of the sperm tail is used as the criterion of the beginning of spermiogenesis.

Shortly before the appearance of tail flagella, each cell of the mass is more or less spherical in shape and measures about 12 μm in diameter; the surface is wrinkled (Fig. 2). As the formation of the sperm tail occurs, the flagellum projects radially from the free surface of each spermatid. Although the main cell body of the spermatid is spherical in shape during early stages of the flagellar formation, it undergoes a gradual elongation with the extension of the tail. At the same time the cell surface becomes smooth. It is of interest to note that a small bulge is always observed on the surface of the region near the proximal terminal of the flagellum (Fig. 3). A similar bulge is also detected on the smooth surface of the flagellum. With the increase in length of the flagellum, a remarkable constriction clearly separates the sperm head from the tail (Fig. 4). The head region is ellipsoidal in shape with a smooth surface and gradually tapers anteriorly. The region near the apex of the head bears a small spherical body which may be an anlage of the acrosome (Fig. 4, arrows). The width of the tail is nearly the same as that of the head and apparently larger than that of the preceding stage. These facts may indicate the occurrence of the distal migration of the spermatid cytoplasm at this stage. In this connection it is of interest to note that the surface of the flagellum is warty in appearance. At the end of spermiogenesis, the cellular mass appears as a swarm of spermatozoa (Fig. 5). Like spermatozoa suspended singly in the male segment, each flagellum of these spermatids shows a distortion in the region near its distal end (Fig. 5, inset).

Spermiogenesis observed by TEM

The occurrence of marked changes in the cell shape of differentiating spermatids was recognized by SEM. In the following description, attention is

mainly concentrated on the nuclear elongation with chromatin condensation and on the formations of the acrosome and the tail flagellum.

Nuclear elongation and chromatin condensation: As described already, each differentiating spermatid attaches to the cytophore through a cytoplasmic bridge which bears fine granules on the inner surface of the plasma membrane and is coated externally by fuzzy material. The round nucleus of the spermatid is surrounded by a dilated nuclear envelope and contains rather diffused chromatins (Fig. 6). The chromatin condensation begins when microtubules are assembled in the perinuclear cytoplasm; it commences on the inner surface of the collapsed nuclear envelope neighboring the cytoplasmic microtubules. The nuclear surface becomes more or less concave in the vicinity of microtubules (Fig. 7). No condensation is observed in the nuclear region partitioned from the cytoplasm by the dilated nuclear envelope, where the nuclear surface is not concave; no microtubules are found in the cytoplasm of this region. As the result of deformation, the nuclear shape at this stage is polygonal. The perinuclear microtubules show a quite regular arrangement in 2 or 3 rows with a distance of 52–60 nm from center to center of individual tubules.

With the increase in area of the nuclear surface characterized by condensed chromatins, the spermatid nucleus is elongated along the length of cytoplasmic microtubules. At the same time, its transverse section reveals a gradual flattening of the nuclear shape as illustrated in Figures 8–10; the lateral surface of the ellipsoidal nucleus is decorated with condensed chromatins. The cytoplasm near the lateral surface of the nucleus contains regularly arranged microtubules which apparently increase in number as chromatin condensation progresses in the nucleus. The nuclear envelope is still dilated at the both ends of the ellipsoidal nucleus where there are no microtubules in the neighboring cytoplasm. In this connection, it is of interest to note that the outer lamina of the dilated nuclear envelope appears to be pinched out into the cytoplasm (Fig. 8, arrows). It is possible that some small vesicles in these spermatids may be produced in this way and then distributed over the cytoplasm. Longitudinal sections of the elongate spermatid reveal that microtubules run along the length of the nucleus without forming a coil around the latter (Fig. 11); in transverse sections, they shows an arrangement in 4 or more rows with a distance of 40–45 nm from center to center of individual tubules. The interval between microtubules therefore apparently decreases.

With a further elongation and flattening of the spermatid nucleus, chromatin condensation proceeds inward. In spermatids with a marked constriction at the boundary between the head and tail (Fig. 4), the entire space of the nucleus is filled with high electron-dense material. The cytoplasm near the flat surface of the nucleus contains a number of microtubules spaced 28–32 nm apart from center to center of individual tubules (Fig. 12). The longitudinal run of microtubules in the elongate spermatids is still obvious. Even at this stage, however, both ends of the ellipsoidal nucleus still lack these tubules.

Golgi apparatus and formation of acrosome: The cytoplasm of early spermatids is characterized by the presence of a prominent Golgi apparatus which consists of a stack of flattened cisternae with neighboring small vesicles (Fig. 6). This apparatus usually lies at the distal portion of the spermatid but it sometimes occurs in the region near the cytoplasmic bridge. There are occasionally accumulations of small vesicles between the nuclear surface and the innermost cisterna of the Golgi apparatus. Careful observations of this region suggest that the pinching off of the outer lamina of the nuclear envelope produces these vesicles (Fig. 13).

The full sequence of the acrosome formation during spermiogenesis is illustrated in Figures 14–21. At the first step of the formation, the outermost cisterna of the Golgi apparatus with dense contents migrates to a position beneath the plasmalemma and ultimately forms a primary acrosomal vesicle. Since the cisterna curves outward in its midregion, it takes the shape of a dome near the cell surface (Fig. 14). There are two dense dots inside the dome. They are sections of a ring which ultimately forms an acrosomal tube. Unfortunately we are not able to elucidate the origin of this ring in this study. Afterwards, the dome discards its peripheral rim and is transformed into a cap-shaped primary acrosomal vesicle (Fig. 15). At the same time, the electron-dense ring increases in height and grows into a tubular body, an acrosomal tube, inside the primary acrosomal vesicle (Fig. 16). When the tube attains a length of about 0.25 μm, its posterior end is closed by a deposit of electron-dense material. Since its anterior end contacts with the posterior surface of the primary acrosomal vesicle, the lumen of the tube is separated from the surrounding cytoplasm (Fig. 17). Probably owing to the presence of the acrosome complex, the surface of the spermatid protrudes outward (Fig. 18); the cytoplasmic bulge of the surface near the proximal terminal of the flagellum, as observed by SEM, may be produced in this manner (Fig. 3). Subsequent to the formation, the acrosome complex migrates toward the proximal region of the spermatid and occupies a position near the cytoplasmic bridge. The axis of the acrosome complex is at first independent of that of the elongate nucleus (Fig. 19). As the perinuclear microtubules extend beyond the anterior level of the elongate nucleus, however, it coincides with the axis of the nucleus; the posterior end of the acrosomal tube achieves a position on the apex of the elongate nucleus (Fig. 20). At the final stage of the acrosome morphogenesis, the primary acrosomal vesicle bends inward considerably, so that the diameter of the dome formed by the vesicle coincides with that of the acrosomal tube (Fig. 21); the acrosome complex is about 0.5 μm long and 0.08 μm wide. Electron-dense material constitutes the contents of the acrosomal vesicle as well as the wall of the acrosomal tube. The bulk of the lumen of the tube is however filled with low electron dense material.

Formation of tail flagellum: A few mitochondria are observed in the cytoplasm of the early spermatid as well as in the cytophore. As microtubules are assembled along the length of the elongating nucleus, most mitochondria migrate toward the cytophore. A pair of mitochondria situated in the distal cytoplasm of the spermatid

however escape from the dislodgement. They contact each other intimately and occupy a position at the distal end of the elongating nucleus to form a nebenkern (Fig. 17). It appears as if they are fixed at the position of the nuclear surface when cytoplasmic microtubules extend posteriorly beyond the level of the nucleus (Fig. 22). Transverse sections through the region immediately behind the nucleus clearly demonstrate that the nebenkern consists of a pair of mitochondria closely adjoined (Fig. 22, inset).

The distal cytoplasm of early spermatids possesses a pair of cylindrical centrioles which are arranged perpendicularly to each other. Immediately after the anchoring of the paired mitochondria at the posterior end of the elongating nucleus, these centrioles are found behind the mitochondria. In the meantime, one of them undergoes degeneration or is discarded from the spermatid (Fig. 11) and the remaining one participates in the formation of the axial filament. There is a narrow space between the centriole and mitochondria. The above mentioned events are observed in the spermatids with diffused chromatins in the nucleus (Fig. 17). Transverse sections of the axial filaments show a typical 9+2 arrangement of microtubules embedded in the granular matrix (Fig. 7); the peripheral 9 doublets derive from the wall of the cylindrical centriole, while the 2 central singlets start at a small "central cylinder" appearing in the lumen of the centriole (Fig. 22). The "central cylinder" measures 70 nm long and 0.1 μm wide; its origin at present is obscure. A high magnification of the section discloses the presence of fibrous structures connecting the central singlets to the peripheral doublets; the appearance resembles a wheel (Figs. 9 and 10). As the elongation of the nucleus proceeds with the extension of perinuclear microtubules, the axis of the cylindrical centriole coincides with that of the nucleus and the space between the centriole and the nebenkern diminishes.

The basic protein transition in spermatid nucleus

It has been observed in various animals that the chromatin condensation in the spermatid nucleus is accompanied by changes in the arginine content of basic proteins. In order to trace the basic protein transition in the nucleus, cytochemical tests were carried out during spermiogenesis of *Tubifex*. Spermatids at the early stage of the differentiation were distinguished by means of light microscopy from those at advanced stages with condensed nucleus; the nucleus of the early spermatid was teardrop-shaped, whereas that with the condensed chromatin was cylindrical. The length of the elongate nucleus was used to determine the final stages of spermatids. In parallel experiments, the same cytochemical tests were employed for the round nuclei of early spermatocytes; the number of cells connecting to the cytophore was used for the distinction of spermatocytes from spermatids (8–64 cells).

The cytochemical results are summarized in Table 1. The nuclei of spermatocytes stain with AFG after TCA or picric acid hydrolysis, indicating the existence of basic proteins within the nuclei. No staining by the same method is,

Table 1. Nuclear basic protein cytochemistry of spermiogenesis in *Tubifex hattai*[1)]

Hydrolysis	Staining	Nucleus			
		spermatocyte	early spermatid[2)]	late spermatid[2)]	spermatozoa[3)]
TCA[4)]	AFG[5)]	+	−	−	−
TCA[4)]	AFG[5)] after deamination	−	−	−	−
Picric acid	AFG[5)]	+	±	+	+
Picric acid	AFG[5)] after acetylation	−	±	+	+
−	Sakaguchi reaction	+	+	++	++

1) Intensity of reaction: ++, intensely positive; +, positive; ±, doubtful; −, negative. 2) Stages were determined by the length of the elongate nucleus. 3) spermatozoa singly suspended in the male segment. 4) TCA, trichloracetic acid. 5) AFG, alkaline fast green.

however, obtained when preparations are previously deaminated or acetylated. It is thus clear that the basophilic nature of the spermatocyte nuclei is principally due to the high content of lysine; the arginine content may be relatively small in these nuclei. The Sakaguchi reaction for arginine is weakly positive in these nuclei. An increase in arginine content of basic proteins following the nuclear elongation is proved by these cytochemical tests. The nuclei of spermatids and spermatozoa do not react to AFG when they are hydrolized by TCA. Since arginine-rich protamines are known to be washed out by TCA treatment, picric acid was used to remove DNA from the nuclei (Bloch and Hew, 1960). After picric acid hydrolysis, the nuclei stain with AFG; they continue to stain even when acetylated. Furthermore, a very intense Sakaguchi reaction is obtained in the cylindrical nuclei. These results indicate that the chromatin condensation in the spermatid nuclei of *Tubifex* is accompanied by the basic protein transition; a considerable increase in arginine content occurs during the nuclear elongation.

Discussion

The sequence of spermiogenesis in *Tubifex* is diagrammatically illustrated in Text-fig. 2. The first sign of sperm differentiation is the formation of the tail flagellum. The free surface of each spermatid extruded a flagellum before the initiation of the acrosome morphogenesis and chromatin condensation. At the first step of the flagellar formation, a pair of cylindrical centrioles arranged perpendicularly to each other were observed at the basal region of the flagellum. In contrast to the cases of other animals (Yasuzumi, 1974), however, the *Tubifex* spermatozoon suspended singly in the male segment contained only one centriole of the pair at this region; another centriole was not detected. The disappearance of a proximal centriole during spermiogenesis has been reported in many oligochaetes, although Gatenby and Dalton (1959) described the persistence of a pair of centrioles in *Lumbricus herculeus* spermatids at an advanced stage of the differentiation. According to Webster and Richards (1977), one of the centrioles

in the early spermatid of *Lumbricillus rivalis* is transformed into "circular body" during spermiogenesis and involved in the formation of the acrosomal tube. A similar observation was also reported by Anderson et al. (1967) in *Lumbricus*

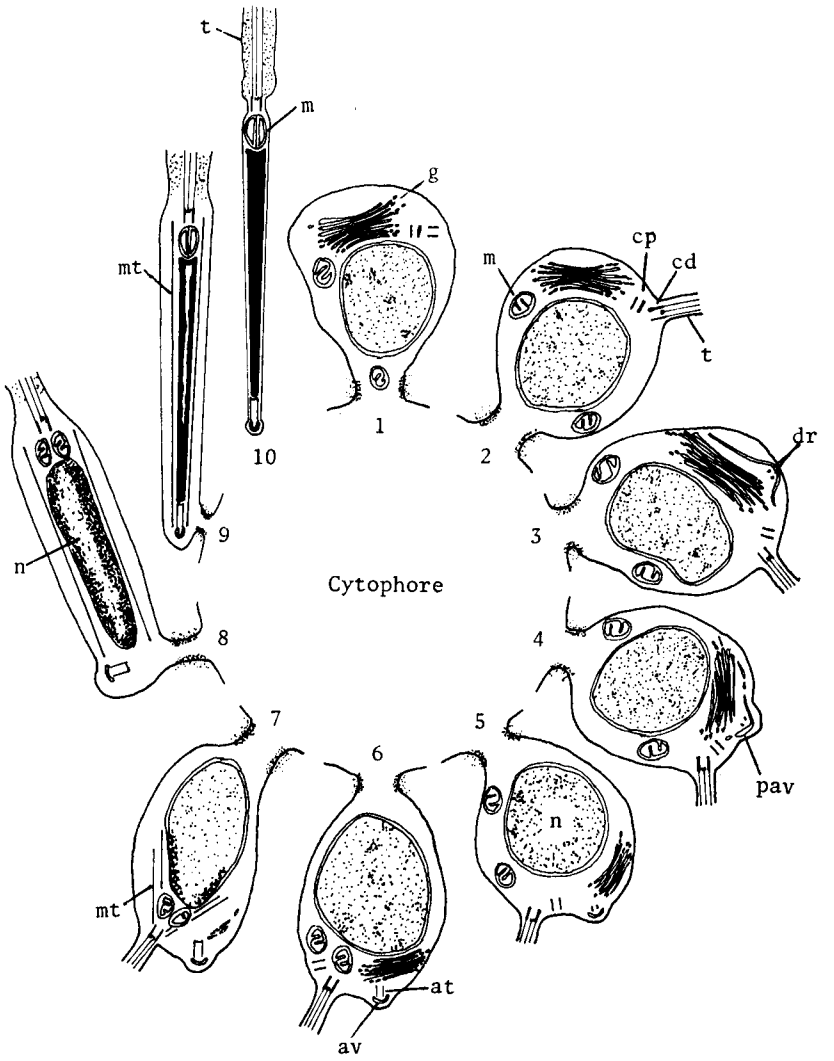

Text-fig. 2. Diagrammatic illustrations showing the sequence of spermiogenesis in *Tubifex hattai*. at, acrosomal tube; av, acrosomal vesicle; cd, distal centriole; cp, proximal centriole; dr, dense ring; g, Golgi apparatus; m, mitochondria; mt, microtubule; n, nucleus; pav, primary acrosomal vesicle; t, tail flagellum.

terrestris. In a recent study of lumbricid spermiogenesis Troyer and Cameron (1980) proposed a different physiological function for the proximal centriole in the spermatids: it participates in the formation of nebenkern at the posterior end of the elongating spermatid nucleus and decreases in size. Eventually the proximal centriole degenerates in the spermatid cytoplasm. Although their fate was not determined exactly in this study, one of the paired centrioles in the *Tubifex* spermatid seems either to degenerate inside or be discarded from the cytoplasm without involvement in the acrosome morphogenesis.

The early spermatid was characterized by the presence of a prominent Golgi apparatus in the distal cytoplasm. According to Stang-Voss (1970), the first cisterna of this apparatus is formed by a pinching off of the outer lamina of the nuclear envelope; through multiplication by folding of this cisterna, a conspicuous Golgi apparatus is formed. An intimate relation of Golgi cisternae to the nuclear envelope has also been suggested for *Tubifex*; in the region between the nuclear surface and the innermost Golgi cisterna, numerous small vesicles were found which were likely to be produced by a pinching off of the outer lamina of the nuclear envelope. The Golgi apparatus, however, was not a newly formed organelle in spermatids; poorly developed Golgi cisternae have been also visible in the cytoplasm of spermatocytes (Troyer and Cameron, 1980: Jaana, unpublished). In view of these facts it is possible to suppose that the prominent Golgi apparatus in spermatids is produced by the addition of cisternae from the nuclear envelope to the poorly developed ones found in the spermatocyte.

The structure of the acrosome complex in *Tubifex* spermatozoa is rather simple. In the spermatozoon suspended singly in the male segment, it consists of the acrosomal vesicle and acrosomal tube, and shows a structural resemblance to that of *Limnodrilus hoffmeisteri* (Block and Goodnight, 1980). The acrosome formation is initiated when the tail flagellum attains a certain length. At this time no sign of the chromatin condensation was appreciated in the spermatid nucleus. The acrosomal vesicle is formed by the Golgi apparatus of the spermatid; the outermost cisterna of the apparatus migrates toward the cytoplasm beneath the free cell surface and is transformed into the primary acrosomal vesicle. A similar origin of the acrosomal vesicle has been described in various species of oligochaetes (Cameron and Fogal, 1963; Reger, 1967; Anderson and Ellis, 1968; Shay, 1972; etc.). As for the acrosomal tube, it is formed through the increase in height of the dense ring which appears inside the dome-shaped primary acrosomal vesicle. The origin of this ring, however, cannot be elucidated in this study. In contrast to the case of enchytraeid, megascolecid and lumbricid (Jamieson and Daddow, 1979), the contents of the acrosomal tube are low electron dense; they are not constructed into the definitive axial rod.

In a light microscopic study of the fertilization of *Tubifex*, Hirao (1968) has observed the formation of a conspicuous fertilization cone on the egg surface near the vegetal pole. Since Henley (1973) has demonstrated the occurrence of an acrosome reaction in the spermatozoa of *Lumbricus terrestris*, it is thought that

the acrosome complex observed in this study shows remarkable changes in structure during fertilization of this worm.

As has been described for many olighochaete species (Ferraguti and Lanzavecchia, 1971; Lanzavecchia and Lora Lamia Donin, 1972; Jamieson and Daddow, 1979; etc.), the chromatin condensation in *Tubifex* spermatids proceeds in parallel with the assembly of microtubules in the perinuclear cytoplasm. These events are initiated when the acrosomal tube attains a certain length. The site of the appearance of microtubules in the cytoplasm was always the vicinity of the nucleus with the concave surface where condensed chromatins were visible. With the increase in area of the nuclear surface which adjoins to the perinuclear cytoplasm with microtubules, the nucleus was flattened laterally and elongated. The transverse section of the nucleus was thus ellipsoidal in shape; both ends of the ellipsoidal nucleus lacked cytoplasmic microtubules, whereas its lateral surface adjoined these tubular components. In spite of considerable activity in microtubule assembly of the perinuclear cytoplasm, the interspace between the plasma membrane and the nuclear surface did not contain such microtubules in spermatozoa suspended individually in the male segment. Since the elongation of the nucleus had been completed in these spermatozoa, the perinuclear microtubules in the spermatids may play a role in the determination of the shape of the sperm head. An external pressure caused by microtubules might be applied to the nucleus and induce the formation of concavity on the nuclear surface as well as its elongation and flattening in differentiating spermatids. Most mitochondria in the cytoplasm of early spermatids migrate toward the cytophore when microtubules are assembled in the perinuclear cytoplasm. This may suggest that the assembly is initiated at the posterior level of the nucleus where the microtubule-organizing centriole exists and proceeds toward the proximal region of the spermatid. Such a directed assembly of microtubules may help the elongation of the nucleus as well as the elimination of cytoplasm from the spermatid. Anderson et al. (1967) proposed for *Lumbricus terrestris* that microtubules generate a motive force for the elimination of both nucleoplasm and cytoplasm. According to Troyer (1980), an active growth of perinuclear microtubules with their attachment to the nuclear envelope and mitochondria in lumbricid spermatids is capable of providing a mechanical force necessary for shaping of the nucleus and the nebenkern. In contrast to these speculations, Fawcett et al. (1971) postulated that shaping of the sperm head is not a consequence of external modeling by pressures applied to the nucleus; it may be determined under the control of genetic material. Since the assembly of perinuclear microtubules must be controlled by the genetic information, it is not surprising that the shape of the sperm head is determined by the effect of microtubules which are controlled by genetic information in the nucleus. It is of interest that the direction of cytoplasmic migration in the differentiating spermatid of *Tubifex* is reversed at late stages of spermiogenesis. Perhaps a distal migration of the cytoplasm may occur in the advanced spermatids, because the width of the tail flagellum increased in the final stages of spermiogenesis. After

completion of the microtubule assembly, the excess cytoplasm around the elongate nucleus may migrate along the length of the microtubules.

The cytochemical results of this study confirm that the basic protein transition in the spermatid nucleus occurs in accord with the progress of the microtubule assembly in the perinuclear cytoplasm. Somatic type histones within the nucleus are replaced by arginine-rich proteins. A similar result was reported for *Lumbricus terrestris* (cf. Bloch, 1969). Ferraguti and Lanzavecchia (1971) and Lanzavecchia and Lora Lamia Donin (1972) postulated a hypothesis that microtubules induce changes of nuclear materials through the collapsed nuclear envelope and indirectly determine the nuclear shape of the spermatozoon. According to Webster and Richards (1977), perinuclear microtubules in *Lumbricillus* spermatids organize protein-binding sites in the inner surface of the nuclear envelope, with which the histones of the chromatin then react in such a way as to facilitate ordered condensation and orientation of the chromatin. It has been proved, however, that in lumbricid spermatids the nucleus once elongated shortens again appreciably (Troyer, 1980). This indicates that chromatin rigidity sufficient to stabilize the shape of the sperm nucleus is obtained during late stages of spermiogenesis. Therefore, chromatin condensation by itself is inadequate for the nuclear shaping; rather, perinuclear microtubules play an important role in the shaping process of the sperm head.

The formation of small vesicles by the nuclear envelope was also observed during chromatin condensation. This might be correlated with the elimination of excess nucleoplasm from the spermatid nucleus. A similar speculation was postulated by Anderson et al. (1967) and Ferraguti and Lanzavecchia (1971). It is therefore possible to suppose that the decrease in volume of the nucleus during spermiogenesis is accomplished by the formation of such vesicles.

Summary

Individual spermatozoa of *Tubifex hattai* are occasionally found in the male segment of the clitellum. Each of them measures about 55 μm long and 0.8 μm wide. The acrosome complex is rather simple in structure and consists of an acrosomal vesicle and a hollow acrosomal tube. The elongate nucleus of the sperm head is flattened laterally and contains highly condensed chromatins. At the posterior end of the nucleus, a pair of mitochondria forms a nebenkern. It is followed by a cylindrical centriole which extends the tail flagellum showing a 9+2 arrangement of microtubules. A conspicuous constriction marks the boundary between the sperm head and tail.

The initiation of spermiogenesis in differentiating spermatids is marked by the formation of the sperm tail. It extends from one of the paired centrioles located in the distal cytoplasm of spermatids. During the extension of the flagellum the other centriole degenerates inside or is discarded from the spermatid cytoplasm.

The acrosome complex is formed by the Golgi apparatus situated in the

distal cytoplasm of spermatids. The formation is initiated when the tail flagellum attains to a certain length; no chromatin condensation is appreciated at this stage. The acrosomal vesicle derives from the outermost cisterna of the Golgi apparatus, while the acrosomal tube derives from a dense ring appearing inside the acrosomal vesicle. No definitive axial rod is detected within the tube.

Microtubules are assembled in the perinuclear cytoplasm when the acrosomal tube attains to about half the length of the fully formed one. They appear to help the proximal migrations of the acrosome complex and excess mitochondria other than those forming nebenkern in the spermatids. The assembly seems to be intimately correlated with the nuclear elongation and chromatin condensation which is accompanied by the nuclear histone transition; nuclear arginine increases in amount during these morphological changes.

The author wishes to express his sincere appreciation to Professor T. S. Yamamoto, Hokkaido University, for his invaluable advice and for improvement of the manuscript.

References

Alfert, M. and I. I. Geschwind 1954. A selective staining method of the basic proteins of cell nuclei. Proc. Nat. Acad. Sci. U.S.A. **39**: 991–999.

Anderson, W. A. and R. A. Ellis 1968. Acrosome morphogenesis in *Lumbricus terrestris*. Z. Zellforsch. **85**: 398–407.

————, Weissman, A. and R. A. Ellis 1967. Cytodifferentiation during spermiogenesis in *Lumbricus terrestris*. J. Cell Biol. **32**: 11–26.

Bloch, D. P. 1969. A catalog of sperm histones. Genetics (Suppl.) **61**: 93–111.

———— and H.W.C. Hew 1960. Changes in nuclear histones during fertilization, and early embryonic development in the pulmonate snail, *Helix aspersa*. J. Biophys. Biochem. Cytol. **8**: 69–81.

Block, E. M. and C. J. Goodnight 1980. Spermatogenesis in *Limnodrilus hoffmeisteri* (Annelida, Tubificidae): A morphological study of the development of two sperm types. Trans. Amer. Micr. Soc. **99**: 368–384.

Bols, N. C. and H. E. Kasinsky 1972. Basic protein composition of anuran sperm: A cytochemical study. Canad. J. Zool. **50**: 171–177.

———— and ———— 1974. Cytochemistry of sperm histones in three cartilaginous fish. *Ibid.* **52**: 437–439.

Braidotti, P. and M. Ferraguti 1982. Two sperm types in the spermatozeugmata of *Tubifex tubifex* (Annelida, Oligochaeta). J. Morph. **171**: 123–136.

Cameron, M. L. and W. H. Fogal 1963. The development and structure of the acrosome in the sperm of *Lumbricus terrestris* L., Canad. J. Zool. **41**: 753–761.

Carver, M. J., Brown, F. C. and L. E. Thomas 1953. An arginine histochemical method using Sakaguchi's new reagent. Stain Tech. **28**: 89–91.

Epel, D. 1978. Mechanisms of activation of sperm and egg during fertilization of sea urchin gametes. Current Topics Develop. Biol. **12**: 185–246.

Fawcett, D. W., Anderson, W. A. and D. M. Phillips 1971. Morphogenetic factors influencing the shape of the sperm head. Develop. Biol. **26**: 220–251.

Ferraguti, M. and G. Lanzavecchia 1971. Morphogenetic effects of microtubules. I.

Spermiogenesis in Annelida Tubificidae. J. Submicr. Cytol. **3**: 121–137.

Gatenby, J. B. and A. J. Dalton 1959. Spermiogenesis in *Lumbricus herculeus*. An electron microscope study. J. Biophys. Biochem. Cytol. **6**: 45–52.

Henley, C. 1973. Ultrastructure of the spermatozoon of the earthworm as revealed by negative staining. J. Morph. **140**: 197–214.

Hirao, Y. 1964. Reproductive system and oogenesis in the freshwater oligochaete, *Tubifex hattai*. J. Fac. Sci. Hokkaido Univ., Ser. VI, Zool. **15**: 439–448.

————. 1968. Cytological study of fertilization in *Tubifex* egg. Zool. Mag. (Tokyo) **77**: 340–346.

Jaana, H. 1982. The ultrastructure of the epithelial lining of the male genital tract and its role in spermatozeugma formation in *Tubifex hattai* Nomura (Annelida, Oligochaeta). Zool. Anz. **209**: 159–176.

Jamieson, B. G. M. 1978. A comparison of spermiogenesis and spermatozoal ultrastructure in megascolecid and lumbricid earthworms (Oligochaeta: Annelida). Austr. J. Zool. **26**: 225–240.

———— 1981. The Ultrastructure of the Oligochaeta. Academic Press, London.

———— and L. Daddow 1979. An ultrastructural study of microtubules and the acrosome in spermiogenesis of Tubificidae (Oligochaeta). J. Ultrastruct. Res. **67**: 209–224.

————, ———— and J. D. Bennett 1978. Ultrastructure of the tubificid acrosome (Annelida, Oligochaeta). Zoologica Scripta **7**: 115–118.

Lanzavecchia, G. and C. Lora Lamia Donin 1972. Morphogenetic effects of microtubules. II. Spermiogenesis in *Lumbricus terrestris*. J. Submicr. Cytol. **4**: 247–260.

Mazia, D., Schatten, G. and W. Sale 1975. Adhesion of cells to surface coated with polylysine. J. Cell Biol. **66**: 190–200.

Reger, J. F. 1967. A study on the fine structure of developing spermatozoa from the oligochaete, *Enchytraeus albidus*. Z. Zellforsch. **82**: 257–269.

Shay, J. W. 1972. Ultrastructural observations on the acrosome of *Lumbricus terrestris*. J. Ultrastruct. Res. **41**: 572–578.

Stang-Voss, C. 1970. Zur Entstehung des Golgi-Apparates. Elektronenmikroskopische Untersuchungen an Spermatiden von *Eisenia foetida* (Annelidae). Z. Zellforsch. **109**: 287–296.

Troyer, D. 1980. Spermiogenesis in lumbricid earthworms revisited. II. Elongation and shortening of the spermatid nucleus and the roles of microtubules and chromatin in organelle shaping. Biol. Cellulaire **37**: 287–292.

———— and M.L. Cameron 1980. Spermiogenesis in lumbricid earthworms revisited. I. Function and fate of centrioles, fusion of organelles and organelle movements. *Ibid.* **37**: 279–286.

Webster, P. M. and K. S. Richards 1977. Spermiogenesis in the enchytraeid *Lumbricillus rivalis* (Oligochaeta: Annelida). J. Ultrastruct. Res. **61**: 62–77.

Yasuzumi, G. 1974. Electron microscope studies on spermiogenesis in various animal species. Int. Rev. Cytol. **37**: 53–119.

Explanation of Plates III - VIII

Abbreviations

ac, acrosome complex; at, acrosomal tube; av, acrosomal vesicle; c, centriole; cb, cytoplasmic bridge; cy, cytophore; dr, dense ring; ep, end piece; g, Golgi apparatus; h, head; m, mitochondria; mt, microtubule; n, nucleus; pav, primary acrosomal vesicle; pp, principal piece; t, tail flagellum.

Plate III

Fig. 1. SEM of the spermatozoon individually suspended in the male segment. Note a conspicuous constriction at the boundary between the head and tail. Bar=5 μm. Inset: High magnification of the head region of the spermatozoon. Note the swelling of the acrosome apex. Bar=1 μm.

Fig. 2. SEM of the mass of round-shaped early spermatids before the formation of tail flagellum. Note the wrinkled surface of the cells. Bar=10 μm.

Fig. 3. SEM of the mass of early spermatids with tail flagellum. The main body of each spermatids is ellipsoidal in shape and bears a small bluge (arrows) on its surface near the flagellum. Bar=2 μm.

Plate IV

Fig. 4. SEM of the mass of spermatids at a late stage of spermiogenesis. A marked constriction exists at the boundary between the head and tail regions. Note a swelling at the region near the apex of each sperm head. Compare the width of the tail flagellum with that shown in Fig. 3. Bar=2 μm.

Fig. 5. SEM of the mass of spermatids at the final stage of spermiogenesis. It appears as if spermatozoa swarm around the center of the mass. Bar=20 μm. Inset: High magnification of the distal portion of the tail flagellum showing the distortion of its course. Bar=5 μm.

Plate V

Fig. 6. Section through the early spermatid with no tail flagellum. The cytoplasm is continuous to the cytophore through a narrow bridge. This stage is characterized by the presence of a prominent Golgi apparatus in the spermatid cytoplasm. Bar=1 μm.

Figs. 7–10. Transverse sections through spermatids showing successive stages of chromatin condensation in the nucleus and the microtubule assembly in the perinuclear cytoplasm. Note the topographical relation of the nuclear dense material and the cytoplasmic microtubules. The nucleus flattens laterally with the increase in number of regularly arranged microtubules. In Fig. 10, the elimination of nucleoplasm by means of the vesicular formation is visible (arrows). Transverse sections through the tail flagella seen in Figs. 9 and 10 show the presence of fibrous structures connecting the central singlets of microtubules to the peripheral doublets. Figs. 7 and 8; Bar=1 μm. Figs. 9 and 10; Bar=0.5 μm.

Plate VI

Fig. 11. Longitudinal section through spermatids at the stage presented in Fig. 9. Note perinuclear microtubules running parallel to the surface of the elongate nucleus without forming a coil around the nucleus. The nebenkern consisting of a pair of mitochondria is fixed at the posterior terminal of the nucleus. One of the paired centriole is distinct but the other indistinct, suggesting its degeneration. Bar=1 μm.

Fig. 12. Transverse section through spermatids at a late stage of spermiogenesis. The chromatin condensation in the nucleus is nearly completed but perinuclear microtubules are still visible in these spermatids. Note the decrease in the interval of microtubules. Bar=0.5 μm.

Fig. 13. Section through the Golgi apparatus of early spermatid. In the cytoplasmic region between the nuclear surface and the innermost cisterna of the apparatus, there are small vesicles which are produced by pinching off (arrows) of the outer lamina of the nuclear envelope. Bar=0.5 μm.

Plate VII

Figs. 14–21. Sections through spermatids showing successive stages of the acrosome formation. The outermost cisterna of the Golgi apparatus migrates toward the cell surface and takes a shape of the dome in Fig. 14. Note sections of the dense ring inside the dome. The rim of the dome is cut off from the rest and the cap-shaped primary acrosomal vesicle is produced in Fig. 15. The dense ring is transformed into the acrosomal tube in Figs. 16 and 17. Note the deposit of electron-dense material at its posterior end. The rudiment of the acrosome complex pushes against the cell surface forming a bulge in the region near the proximal end of the tail flagellum (Fig. 18). It migrates toward a region opposite to the basal centriole of the tail flagellum (Fig. 19) and achieves a position at the anterior end of the elongate nucleus (Fig. 20). The perinuclear microtubules running parallel to the elongate nuclear surface laterally support the rudiment of the acrosome complex. In Fig. 21, the primary acrosomal vesicle bends inward considerably and closes the anterior end of the acrosomal tube. Figs. 14–16 and Figs. 18–21; Bar=0.5 μm. Fig. 17; Bar=1 μm.

Plate VIII

Fig. 22. Longitudinal section through a spermatid showing the support of nebenkern by perinuclear microtubules extending posteriorly beyond the level of the nucleus. Note the "central cylinder" (arrow) at the beginning of the central singlets of the tail flagellum. Bar=1 μm. Inset: Transverse section through the region immediately behind the elongate nucleus of a spermatid showing that a pair of mitochondria constitute the nebenkern. Bar=1 μm.

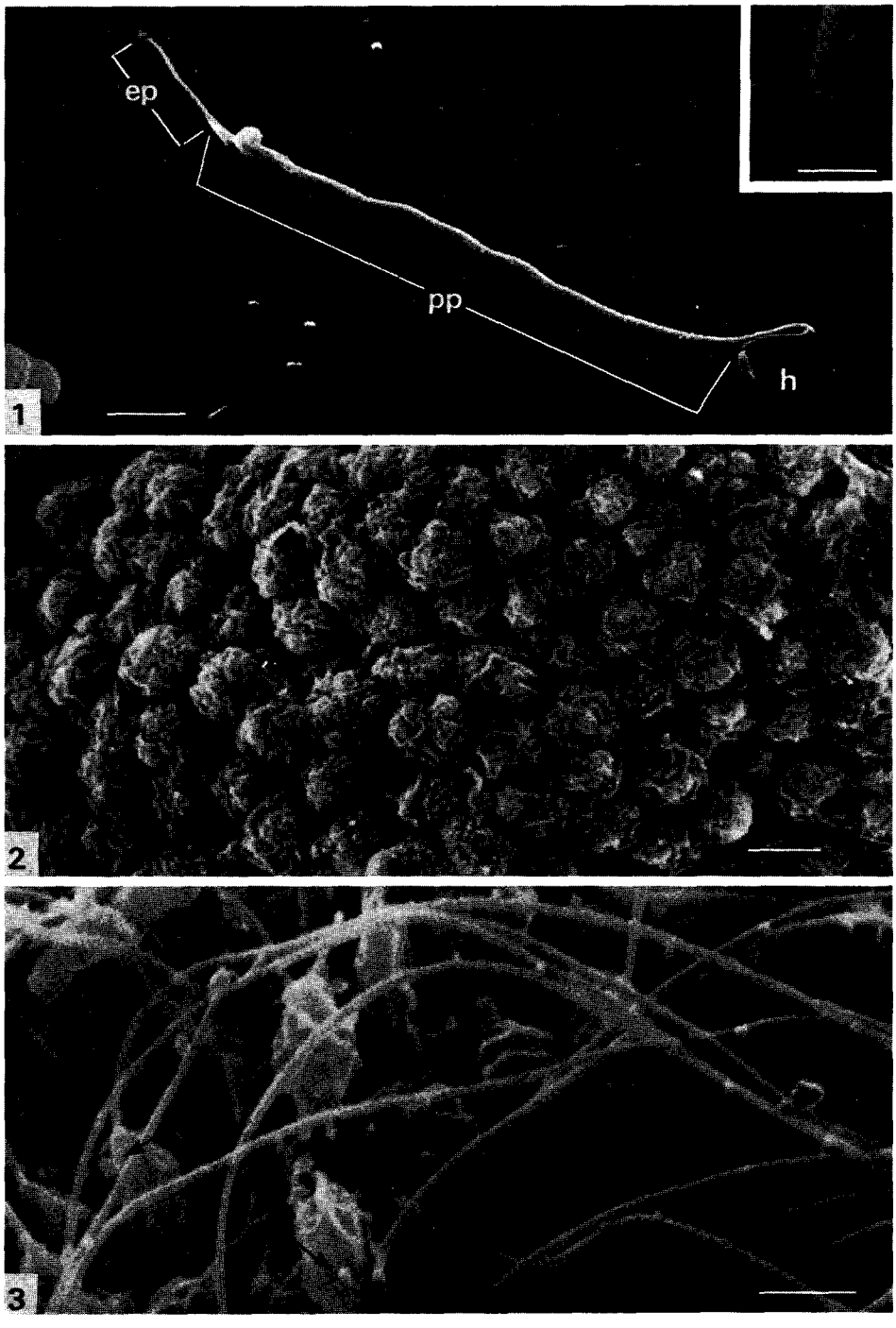

H. Jaana: *Spermiogenesis in* Tubifex hattai

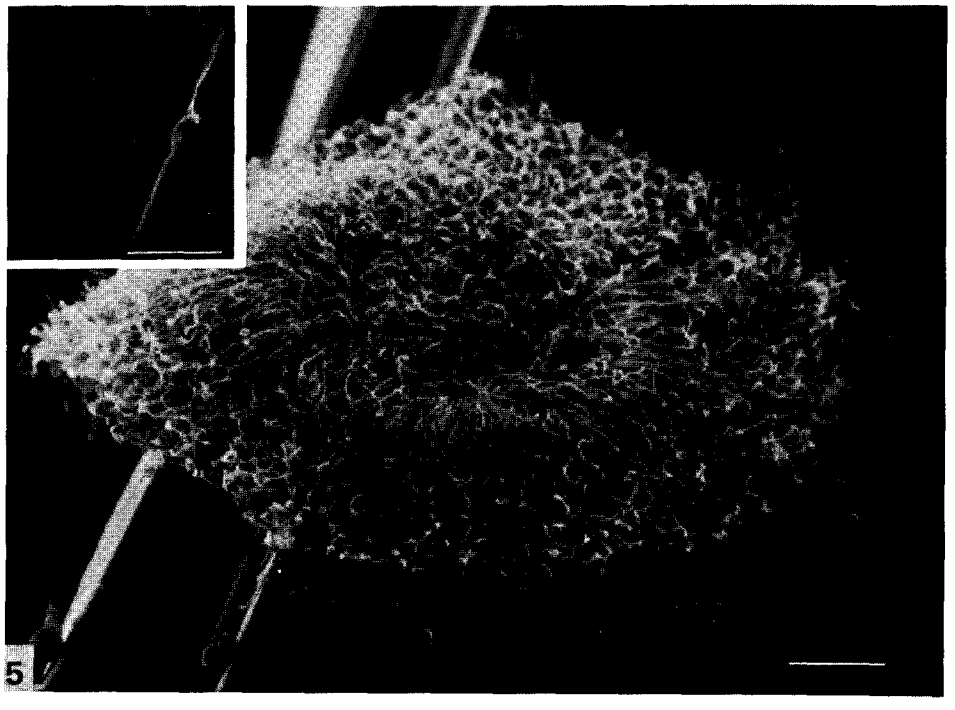

H. Jaana: *Spermiogenesis in* Tubifex hattai

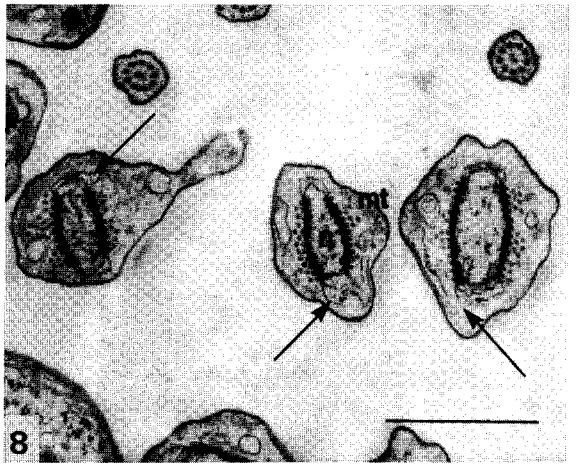

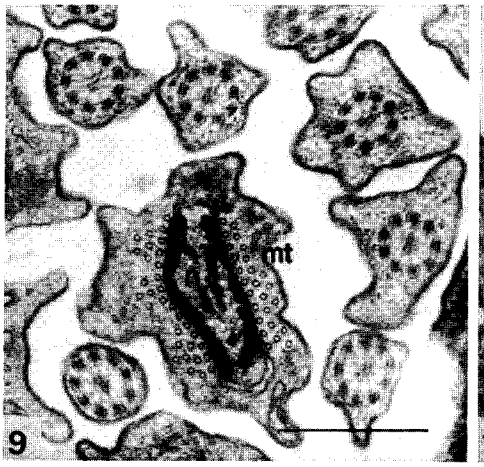

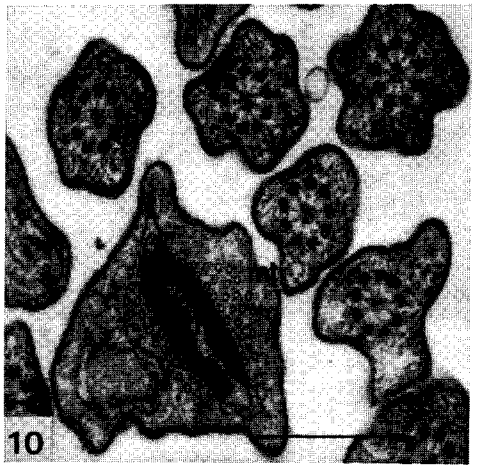

H. Jaana: *Spermiogenesis in* Tubifex hattai

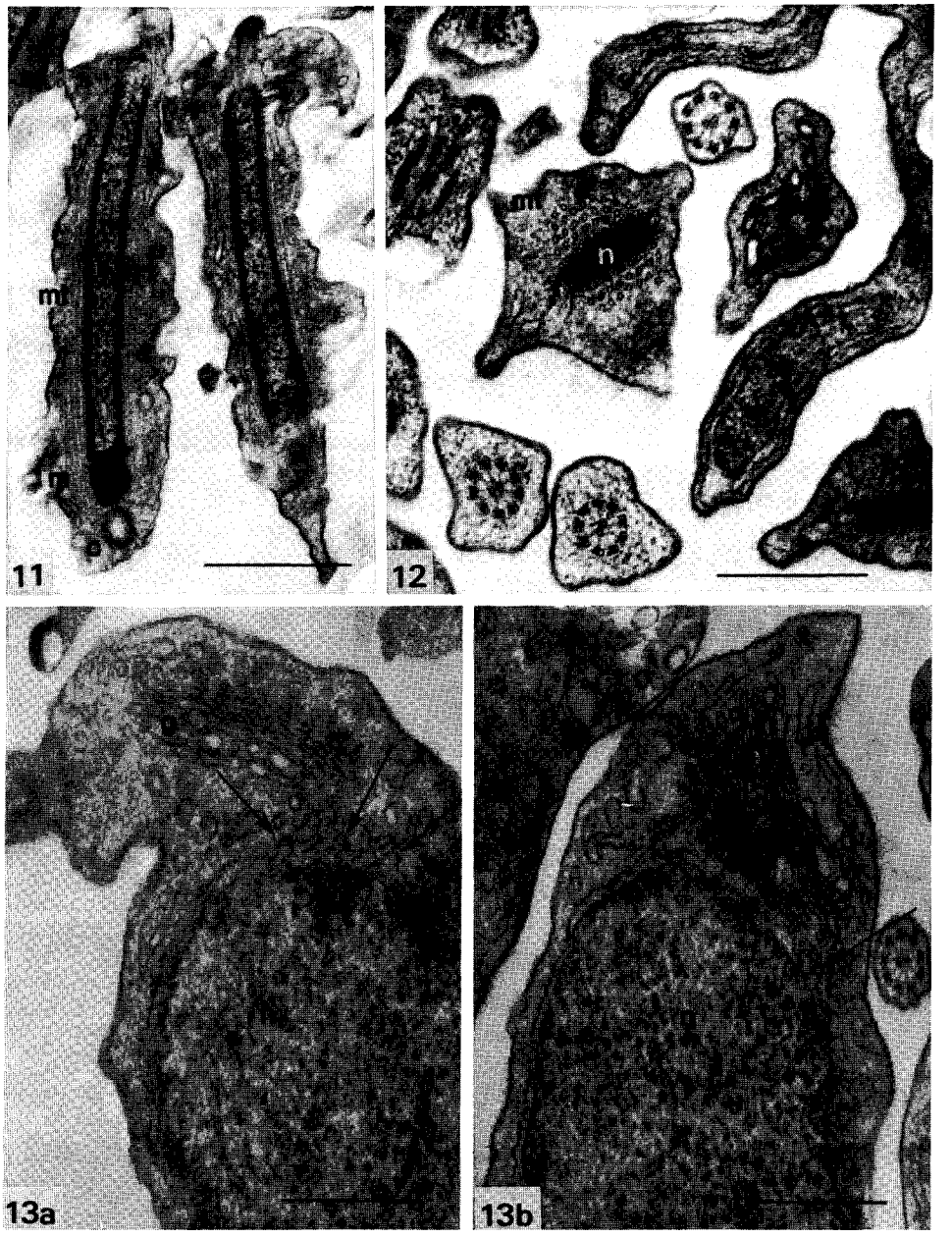

H. Jaana: *Spermiogenesis in* Tubifex hattai

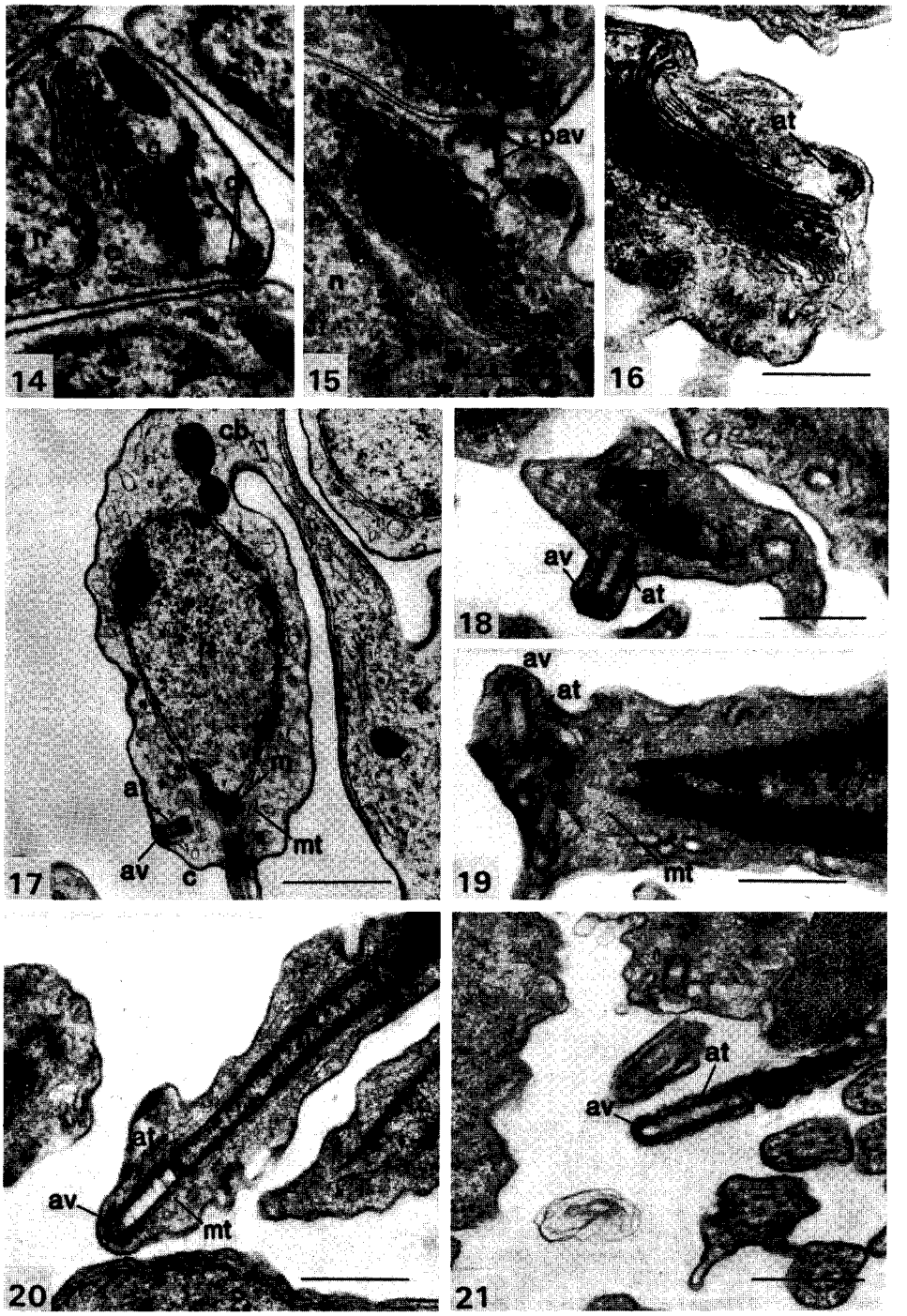

H. Jaana: *Spermiogenesis in* Tubifex hattai

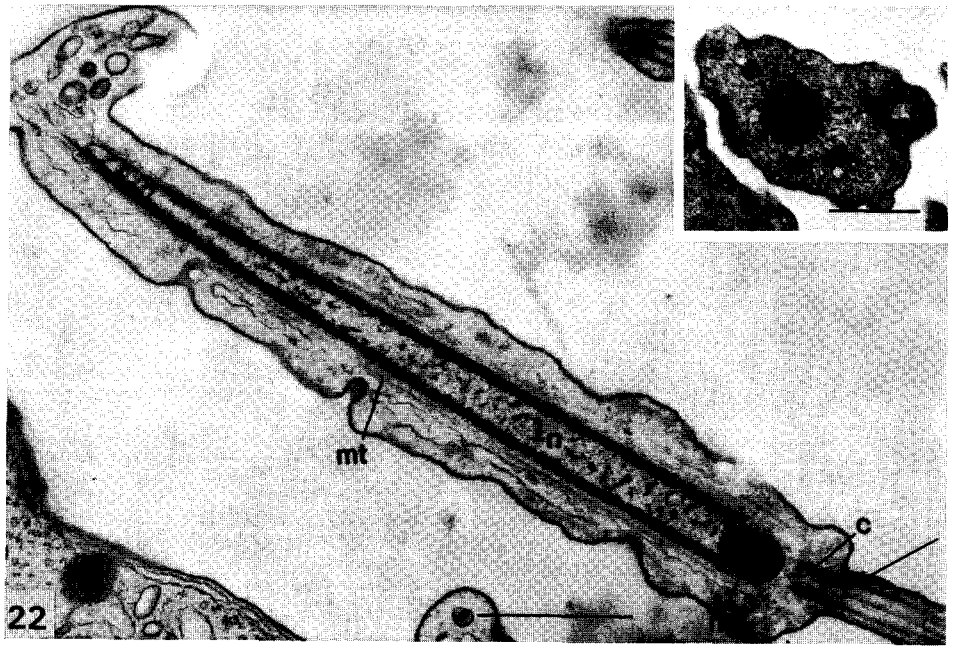

H. Jaana: *Spermiogenesis in* Tubifex hattai